J. Am. Ceram. Soc., 96 [8] 2362–2365 (2013)
DOI: 10.1111/jace.12468

journal
Rapid Communication

Characterizing Weave Geometry in Textile Ceramic Composites Using Digital Image Correlation

Michael N. Rossol,[‡] John H. Shaw,[‡] Hrishikesh Bale,[§,¶] Robert O. Ritchie,[§,¶] David B. Marshall,[‖] and Frank W. Zok[‡,†]

[‡]Materials Department, University of California, Santa Barbara, California 93106

[§]Department of Materials Science and Engineering, University of California, Berkeley, California 94720

[¶]Materials Science Division, Lawrence Berkeley National Laboratory, Berkeley, California 94720

[‖]Teledyne Scientific Company, Thousand Oaks, California 91360

Techniques for characterizing tow architectures and defects in woven ceramic composites are required for generating high-fidelity geometric models and subsequently probing effects of defects on composite performance. Although X-ray computed tomography (CT) has been shown to provide the requisite information with potentially sub-μm resolution, the technique is inherently limited to probing only small volumes: on the order of a few unit cells of typical weaves. Here, we present an assessment of the efficacy of a complementary 2D technique, based on surface topography mapping via 3-D (three-dimensional) digital image correlation (DIC), with potential for ascertaining long-range features in weaves and defects that cannot be gleaned from CT imaging alone. Upon comparing surfaces reconstructed from CT and DIC data, we find that DIC is capable of resolving surface heights with a root mean square(RMS) error of ~10 μm (about twice the CT voxel size, 4.4 μm) and a spatial resolution of ~20 μm over areas of several cm^2. Achieving this level of resolution requires use of sufficiently small speckles (~50 μm) and small subset size (~300 μm) relative to the characteristic tow dimensions (~1 mm). The error is somewhat higher (about 20 μm) in areas where surface discontinuities or rapid changes in topography exist (e.g., at tow boundaries).

I. Introduction

Digital image correlation (DIC) has become a common tool for measuring in-plane displacement and strain fields on surfaces of materials subjected to mechanical or thermal loads.[1–3] In the context of fiber-reinforced ceramic composites (CMCs), DIC has been used to probe the effects of tow architecture on local strain variations at ambient[4] and elevated temperatures.[5] When combined with stereo imaging, DIC also yields out-of-plane displacements as well as surface topography, though the latter capability has not been exploited extensively in the ceramics community.[1,3–6]

The objectives of the present communication are twofold: (i) to demonstrate the utility of 3D DIC for high-resolution characterization of fiber tows in thin, woven, partially densified C/SiC preforms, and (ii) to critically assess the resolution of such measurements through direct comparisons with results obtained from synchrotron X-ray computed tomography (CT).[7–10] The comparisons are used to compute measurement errors and their dependence on the DIC analysis parameters.

Although DIC measurements are inherently two-dimensional in nature, the external surfaces of the composites of present interest (described below) constitute a significant fraction of all tow surfaces. Consequently, we expect the technique to provide substantial information (though clearly not comprehensive) on geometric tow defects that cannot be gleaned from CT imaging alone. Its use in probing large areas will be the focus of a forthcoming publication.

II. Materials and Experimental Methods

The material of interest is a woven three-layer angle interlock C–SiC composite.[8–10] The fiber preform consists of T300-6K tows in the configuration depicted in Fig. 1. The fibers (each of diameter 7 μm) had been coated with a thin layer of pyrolytic carbon (as a debond layer) via chemical vapor infiltration (CVI). The preform was then partially infiltrated with CVI SiC, resulting in a 40 μm-thick matrix layer around the fiber tows. The tows are approximately elliptical in cross section (~1 mm × 0.2 mm). The surface of the CVI SiC surrounding each tow is textured with fine striations (~100 μm wide) replicating positions of underlying fibers. In this (partially processed) state, the fiber tow boundaries can be readily discerned in the synchrotron images and the external surfaces of the panel present an accurate depiction of the local tow positions.

The results of CT imaging have been presented elsewhere.[8–10] The test specimen had been imaged using monochromatic X-rays with 21 keV energy at the Advanced Light Source (Lawrence Berkely National Laboratory, Berkeley, CA). The specimen was 1.3 mm thick and 8 mm wide. Five tiled scans covering a height of 13 mm were conducted. The specimen comprised the equivalent of about two unit cells of the fiber weave. A commercial reconstruction code (Octopus v8, IIC Ugent, Belgium) was used to create a set of two-dimensional slices normal to the rotation axis. The surfaces of the sample were identified by binarizing each two-dimensional slice to maximize contrast between the sample surface and the background and then locating the outermost pixels with a value not equal to that of the background. Visualization of reconstructed surfaces and associated computations were performed using Mathematica® (Wolfram Research, Champaign, IL).

Both surfaces of the same test coupon were characterized by DIC using procedures presented elsewhere.[4] High-contrast

D. J. Green—contributing editor

Manuscript No. 33121. Received April 29, 2013; approved May 29, 2013.
†Author to whom correspondence should be addressed. e-mail: zok@engineering.ucsb.edu

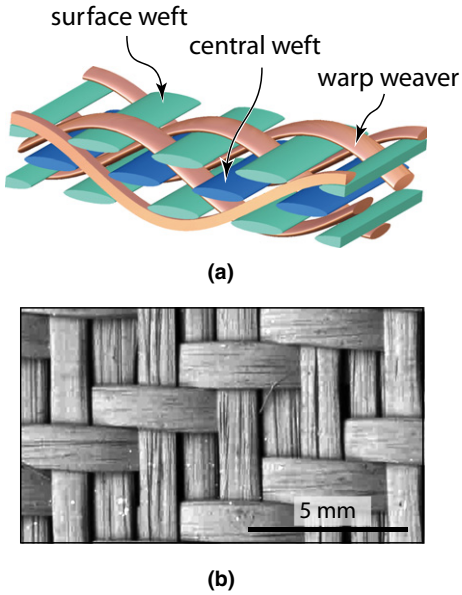

Fig. 1. (a) Schematic and (b) optical image of the three-layer angle interlock weave C–SiC composite.

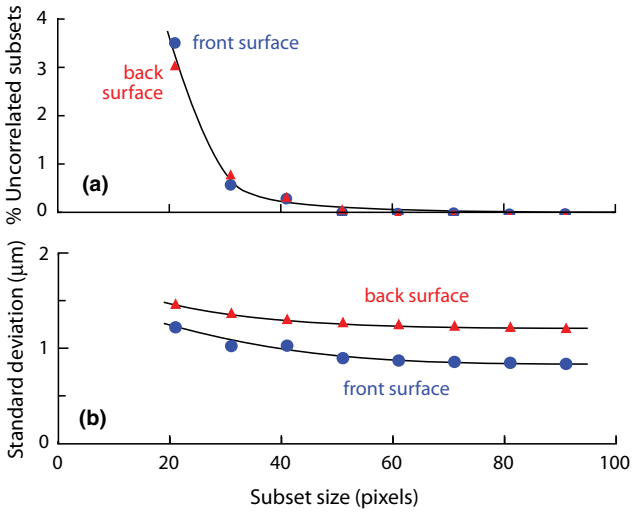

Fig. 2. Effects of subset size on (a) percentage of uncorrelated subsets and (b) standard deviation in surface heights from sequential images.

speckle patterns were produced on the (black) specimen surface using an airbrush with white water-soluble paint. The average speckle size, determined by the autocorrelation technique,[4] was approximately 50 ± 10 μm. Images for DIC were acquired using two digital cameras (Point Grey Research Grasshopper, Richmond, BC, Canada), each with a CCD resolution of 2448 × 2048 pixels and a 70–180 mm lens (Nikon ED AF Micro Nikkor, Nikon Inc., Melville, NY). The experimental setup and imaging conditions were selected to ensure that the entire coupon surface was in the focal plane of both cameras and that the highest possible magnification was attained. To achieve these goals, the lens focal length was 180 mm, the aperture setting was F-22, the magnification was 10 μm/pixel, and the angle between cameras was 19°. Image correlation was carried out using Vic-3D software (Correlated Solutions, Columbia, SC), employing the smallest possible step size (2 pixels, 20 μm) and subset sizes ranging from 21 to 91 pixels. The latter range was selected to assess the trade-offs between spatial resolution and degree of correlation. The intrinsic noise in the height measurements was characterized by the root mean square (RMS) difference between height measurements, obtained from sequential image pairs that had been taken without altering imaging conditions. Variations in degree of correlation and RMS error with subset size (plotted in Fig. 2) reveal a near-optimal subset size of 31 pixels, whereupon 99% of subsets are successfully correlated and the RMS error is 1–1.5 μm (smaller than the CT voxel size: 4.4 μm). As demonstrated below, this noise level is about an order of magnitude lower than the RMS differences between surface heights obtained by DIC and CT. Increasing the subset size yields negligible benefit in terms of improved correlation or noise reduction. On the contrary, as shown below, it leads to increased errors in surface height measurements. Consequently, most results presented subsequently are based on correlations made with this subset size.

To perform quantitative comparisons, the coordinates defining the surface profiles obtained by each of the two techniques were aligned with one another using the locations of the peaks of the warp crowns as fiducial markers. The translations and rotations about the principal axes needed to align the data sets were determined by minimizing the sum of the squares of the Euclidean distances between the peaks of the warp crowns obtained from CT and DIC measurements. The standard deviation in warp crown heights from CT and DIC following alignment was 3.7 μm. Assessments of the DIC technique were made on the basis of 3D render-

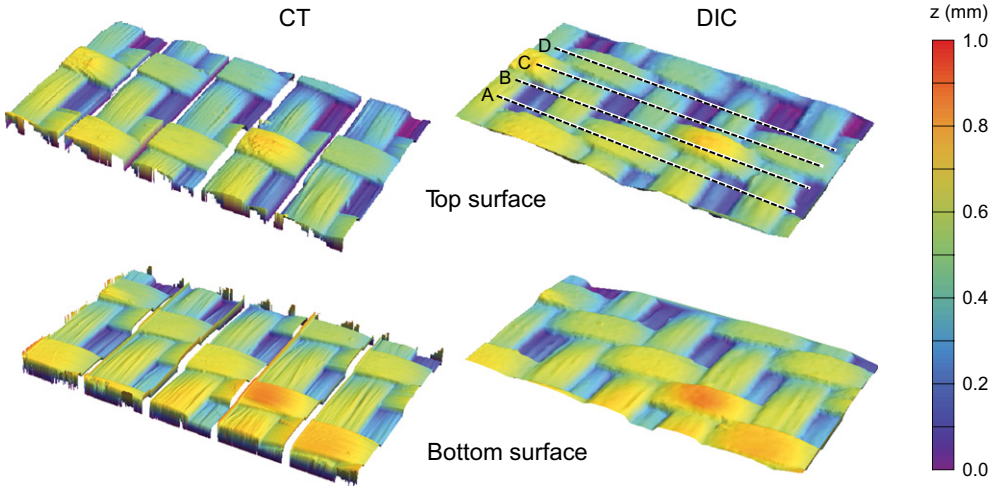

Fig. 3. Comparisons of 3D renderings of surfaces obtained from both CT and DIC. Specimen length (from left to right) is 13 mm. Lines labeled A–D are trajectories of scans presented in Fig. 4. (Narrow gaps between the five tiled scans in the CT images on the left represent regions in which CT data had not been collected.).

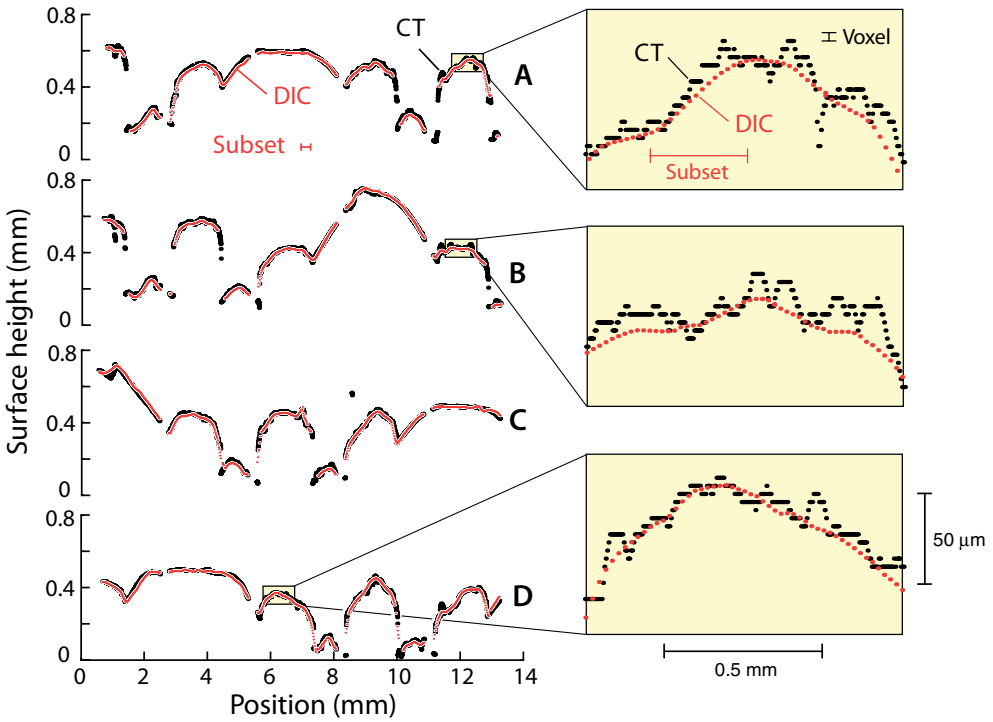

Fig. 4. Representative line scans of surface heights obtained from DIC and CT. Locations of scans A–D are indicated on Fig. 3. Expanded regions on the right are examples where correspondence between DIC and CT is poorer than average, due to the presence of protruding filaments on the composite surface.

ings of the surfaces, line scans of surface heights and residuals between the two data sets.

III. Reconstructed Surfaces

Three-dimensional renderings of reconstructed surfaces from both CT and DIC are shown in Fig. 3. Qualitatively the DIC results appear to provide an excellent representation of the sample surface, as determined by CT, with the exception of the fine surface striations. The inability to capture the striations is due largely to the combination of attainable speckle size (50 μm) and subset size (31 pixels, 310 μm) needed to attain full correlation.

Quantitative comparisons between the two surfaces are presented in the form of line scans of surface heights in Fig. 4. Here, we find that, in regions further than ~100 μm from the boundaries between adjacent tows, the differences are typically <20 μm. Closer to the boundaries, where the surfaces exhibit rapid changes or discontinuities in height, the differences between CT and DIC are somewhat greater, but still typically <50 μm.

A more comprehensive assessment of the fidelity of the DIC-derived surfaces was made by computing the RMS errors σ over the entire surface (comprising > 200 000 data points) over a subset size range 21–91 pixels (Fig. 5). The error was computed in two ways. The first was based on *all* surface data. In the second, a *subset* of those surface regions located more than 0.15 mm from a tow boundary was isolated and analyzed accordingly. The isolated regions for the latter case and the RMS errors are shown in Fig. 5. Neglecting the boundaries, the error is essentially constant, at ~10 μm, up to a subset size of 50 pixels (0.5 mm). This level of error is only about twice the CT voxel size—the latter setting the accuracy on the baseline "true" surface heights. Including the entire surface yields somewhat higher errors at small subset sizes (e.g. 20 μm at a subset size of 31 pixels) and a progressive increase in error with subset size (approximately linear): differences attributable to errors in resolving tow boundaries.

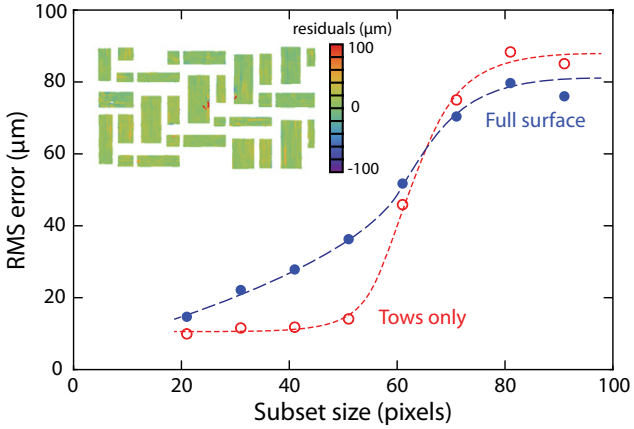

Fig. 5. Variation in RMS error with subset size and, in inset, map of residuals between CT and DIC surfaces for regions away from the tow boundaries, all for a subset size of 31 pixels.

The main sources of error in the preceding comparisons include: (i) the spatial resolution of the CT (roughly half the voxel size: ~2 μm); (ii) the intrinsic noise in the DIC images (~1 μm); (iii) the disregistry between the DIC and CT images (~4 μm); and (iv) the spatial resolution of the DIC measurements and the associated "smoothing" of fine surface features (i.e., curvature of tows and fine surface striations). Although the convolution of these effects in overall measurement error is complex, it would appear that, based on addition of variances, a measurement error of 10 μm is likely to be the best one could expect to achieve from such experiments with analysis areas of several cm^2.

IV. Conclusions

We have demonstrated that, with appropriate selection of test and analysis parameters, 3D DIC measurements based on optical micrographs can resolve the surface topography of

woven CMCs with a height resolution ~10 μm—only about twice the voxel size of CT data used to establish the reference surfaces—and a spatial resolution of about 20 μm. The utility of large-area topographic maps (obtained by stitching together multiple high-resolution maps) in ascertaining long-range defects in tow architecture will be presented in a forthcoming article.

Acknowledgments

This work was supported by the US AFOSR (Ali Sayir) and NASA (Anthony Calomino) under the National Hypersonics Science Center for Materials and Structures (AFOSR Prime Contract No. FA9550-09-1-0477 to Teledyne Scientific and Subcontract No. B9U538772 to UCSB and to UCB). The use of the X-ray microtomography beam line (8.3.2) at the Advanced Light Source.

(Lawrence Berkeley National Laboratory) was supported by the Office of Science of the U.S. Department of Energy under contract no. DE-AC02-05CH11231. The authors also gratefully acknowledge fruitful discussions with Varun Rajan (UCSB).

References

[1]M. Sutton, S. McNeill, J. Helm, and Y. Chao, "Advances in Two-Dimensional and Three-Dimensional Computer Vision," *Photomechanics*, **77**, 323–72 (2000).

[2]M. A. Sutton, J. Yan, X. Deng, C.-S. Cheng, and P. Zavattieri, "Three-Dimensional Digital Image Correlation to Quantify Deformation and Crack-Opening Displacement in Ductile Aluminum Under Mixed-Mode I/III Loading," *Opt. Eng.*, **46** [5] 1–16 (2007).

[3]M. A. Sutton, J.-J. Orteu, and H. W. Schreier, *Image Correlation for Shape, Motion, and Deformation Measurements*. Springer, New York, NY, 2009.

[4]V. P. Rajan, M. N. Rossol, and F. W. Zok, "Optimization of Digital Image Correlation for High-Resolution Strain Mapping of Ceramic Composites," *Exp. Mech.*, **52** [9] 1407–21 (2012).

[5]M. D. Novak and F. W. Zok, "High-Temperature Materials Testing with Full-Field Strain Measurement: Experimental Design and Practice," *Rev. Sci. Instrum.*, **82** [11] 115101 (2011).

[6]S. R. McNeill, M. A. Sutton, Z. Miao, and J. Ma, "Measurement of Surface Profile Using Digital Image Correlation," *Exp. Mech.*, **37** [1] 13–20 (1997).

[7]D. B. Marshall and B. N. Cox, "Integral Textile Ceramic Structures," *Annu. Rev. Mater. Res.*, **38**, 425–43 (2008).

[8]H. Bale, M. Blacklock, M. R. Begley, D. B. Marshall, B. N. Cox, and R. O. Richie, "Characterizing Three-Dimensional Textile Ceramic Composites Using Synchrotron X-ray Micro-Computed-Tomography," *J. Am. Ceram. Soc.*, **95** [1] 392–402 (2012).

[9]M. Blacklock, H. Bale, M. R. Begley, and B. N. Cox, "Generating Virtual Textile Composite Specimens Using Statistical Data From Micro-Computed Tomography: 1d Tow Representations for the Binary Model," *J. Mech. Phys. Solids*, **60** [6] 451–70 (2012).

[10]R. G. Rinaldi, M. Blacklock, H. Bale, M. R. Begley, and B. N. Cox, "Generating Virtual Textile Composite Specimens Using Statistical Data From Micro-Computed Tomography: 3d Tow Representations," *J. Mech. Phys. Solids*, **60** [8] 1561–81 (2012). □